31st Annual International Conference of the IEEE EMBS
Minneapolis, Minnesota, USA, September 2-6, 2009

# Support vector machine classification of complex fMRI data

Scott J. Peltier, Jonathan M. Lisinski, Douglas C. Noll, Stephen M. LaConte

*Abstract*—**This work examines support vector machine (SVM) classification of complex fMRI data, both in the image domain and in the acquired k-space data. We achieve high classification accuracy using the magnitude data in both domains. Additionally, we maintain high classification accuracy even when using only partial k-space data. Thus we demonstrate the feasibility of using kspace data for classification, enabling rapid realtime acquisition and classification.**

## I. Introduction

Pattern classification techniques offer a new way of analyzing imaging data. These methods have been applied in MR imaging using support vector machines (SVM) [1], and have been used to attain real-time feedback [2]. So far, these techniques have been applied in image space. This study explores applying SVM techniques directly on the acquired k-space data.

## II. Methods

### A. MR data acquisition

Data were acquired for four subjects on a 3 T GE scanner. T2*-weighted data was acquired using a spiral-in sequence (TR/TE/FA/FOV=2s/30ms/90/22cm, 64x64 matrix, 3mm slice thickness). A motor task paradigm was used, with alternating blocks of left and right hand finger tapping (20 s each condition per cycle, 8 cycles total, 320 s total time). Forty axial slices were prescribed, and two runs were acquired.

### B. fMRI Classification with Support Vector Machines

As described in [1] classification algorithms attempt to find a decision rule that uses an input vector, $\vec{u}$, to obtain a scalar-valued output class label, $v$. When there are two classes (which is the case considered in this work), the class label can take two values $v \in \{-1,+1\}$. The process of estimating the decision rule is called induction or supervised learning, and uses a training data set $\{\vec{u}_r, v_r\}_{r=1,R}$ with a finite number of examples, *R*. Once the decision rule is determined, test data, consisting of input vectors can be classified by their output values.

The support vector machine (SVM) is one method for classification used in recent fMRI studies [1-2]. For two classes, the SVM algorithm attempts to find a linear decision boundary (separating hyperplane) using the decision function

$$D(\vec{u}_r) = (\vec{w} \cdot \vec{u}_r) + w_0, \quad (1)$$

where $\vec{w}$ defines the linear decision boundary, and is chosen to maximize the boundaries defined by D = +1 and D = -1 (known as the margin) between the two class distributions.

For fMRI, brain state classification uses the experimental design as the class label (e.g. stimulus A and stimulus B are assigned unique classes) and an experiment consists of a series of brain images being collected while class labels are changed. The classifier's input vector consists of an appropriate representation of the spatiotemporal image data. In this situation, we have labeled data.

For block design data, it is possible to represent each image as an input vector $\vec{u}$, as described in [1-2] where the vector components are the intensity values for each brain voxel at the acquisition time. The experimental condition (behavioral state) associated with each $\vec{u}$ defines the class label, $v$. Note that the training data and testing data are assumed to be spatially and temporally aligned and have the same dimensionality.

### C. Complex kernel approach

For complex valued data, our approach was use the complex dot product

$$\vec{w} \cdot \vec{u} = \sum_{n=1}^{N} u_n^* w_n, \quad (2)$$

where N is the number of voxels in the complex image $\vec{u}$, and $u^*$ denotes the complex-conjugate.

Summary maps for complex-valued input data were obtained by the direct visualization of the weight vector as described in [1]. Given complex-valued input vectors several maps are possible:

real

$$\vec{w}^{re} = \sum_{t=1}^{T} \alpha_t v_t \vec{u}_t^{re}, \quad (3)$$

Manuscript received April 23, 2009. This work was supported in part by the NIH grants R21 DA026077 (S.P.) and R21 DA026086 (S.L).

S. J. Peltier is with the Functional MRI Laboratory, University of Michigan, Ann Arbor, MI 48109 USA (phone: 734-647-8077; fax: 734-936-4218; e-mail: spelt@umich.edu).

J. M.. Lisinski is with the Biomedical Engineering Department, Baylor College of Medicine, Houston, TX 77005 USA. (e-mail: jlisinski@)cpu.bcm.edu).

D. C. Noll is with the Biomedical Engineering Department, University of Michigan, Ann Arbor, MI 48109 USA. (e-mail: dnoll@umich.edu).

S. M. LaConte is with the Biomedical Engineering Department, Baylor College of Medicine, Houston, TX 77005 USA (e-mail: slaconte@cpu.bcm.edu).

imaginary

$$\vec{w}^{im} = \sum_{t=1}^{T} \alpha_t \nu_t \vec{u}_t^{im} \ , \quad (4)$$

magnitude

$$\vec{w}^{mag} = \sum_{t=1}^{T} \alpha_t \nu_t \sqrt{\left(\vec{u}_t^{re}\right)^2 + \left(\vec{u}_t^{im}\right)^2} \ , \quad (5)$$

and phase maps

$$\vec{w}^{pha} = \sum_{t=1}^{T} \alpha_t \nu_t \arctan\left(\frac{\vec{u}_t^{im}}{\vec{u}_t^{re}}\right) \ , \quad (6)$$

of the weight vector $\vec{w}$. Here, $\nu_t$ are the real-valued experimental design values (data labels), and $\alpha_t$ are the real-valued Lagrange multipliers solving the SVM problem.

### *D. Implementation and data analysis*

Both SVM training and testing were done using the *3dsvm* command [1] in AFNI [3]. For classification of complex-valued input data, the capabilities of 3dsvm were extended to perform classification with a complex kernel as described in the previous section. Classification was performed on run 2 using run 1 as a training data set, and vice versa, and the two accuracy estimates were averaged. Specifically, percent classification accuracy was calculated as [(number of correctly classified images)/(total number of images) × 100]. Classification was done on the magnitude, phase, and complex data in both image space and k-space. In addition, the dependence on k-space coverage was investigated by examining the classification accuracy when using subsets of magnitude k-space.

## III. Results

Figure 1 displays the SVM model weights using the magnitude image data for six slices covering the primary motor cortex. As expected, the significant model weights are located in the primary motor and supplementary motor cortex.

Figure 2 shows the significant model weights using magnitude k-space data, for the six motor slices. Figure 3 displays all the model weights plotted on the spiral trajectory. More significant model weights are located in centrally in k-space.

The SVM classification results are shown in Table I and Figure 4. Classification using the image magnitude or k-space magnitude data was very high (98% and 87% , respectively, averaged over both train-test permutations). The results using the full-kspace (blue) or only the central 8$^{th}$ of k-space (green) are very similar, with high classification accuracy (87%, 86%), but the accuracy and sensitivity is degraded when using the outer 8$^{th}$ of k-space (red, 75% accuracy). In addition, the classification accuracy is degraded when using the complex image data (65%).

## IV. Discussion

The accuracy was very high in both magnitude k-space and image data. Thus, using k-space data for fMRI classification is feasible, eliminating the need for image reconstruction. This can allow for speed-ups in realtime fMRI (rtfMRI) applications.

The decreased accuracy in the complex data could be due to noise present in the phase data. Two main sources for this are drifts in the field over time, and modulation of the phase due to physiological noise (particularly respiration). It is important to also note that no preprocessing was performed on these data for this study. In general, we expect classifier performance could be improved by correcting for motion and physiological noise. Further work will be done to examine the impact of preprocessing choices on complex-valued fMRI classification.

The ability to achieve high classification accuracy with only partial k-space coverage can enable faster acquisition approaches. By sacrificing spatial resolution, increased temporal resolution can be obtained. We will investigate these tradeoffs in ongoing work.

## V. Conclusions

High classification accuracy was obtained using magnitude image and k-space data. In addition, reduced k-space coverage covering central k-space maintained a high level of accuracy. This can potentially enable rapid real-time classification, without the need for image reconstruction.

## References


[1] S.M. LaConte, S. Strother, V. Cherkassky, X.P. Hu. *NeuroImage*, vol 26, pp. 317-329, 2005.

[2] S.M. LaConte, S.J. Peltier, and X.P. Hu, X.P. (2007), "Real-time fMRI using brain state classification," *Human Brain Mapping,* vol. 28, pp. 1033-44, 2009.

[3] R.W. Cox. (1996) "AFNI: software for analysis and visualization of funtional magnetic resonance neruoimages," *Comp. and Biomed. Res*, vol. 29, pp. 162-173, 1996.

TABLE I. SVM Classification Results

| Subject | Image Magnitude | Image Phase | Image Complex | K-space Magnitude | K-space Phase | K-space Complex | Mag. K-space Inner 8th | Mag. K-space Outer 8th |
|---|---|---|---|---|---|---|---|---|
| **1** | 0.98 | 0.53 | 0.93 | 0.98 | 0.66 | 0.91 | 0.98 | 0.74 |
| **2** | 0.95 | 0.59 | 0.92 | 0.92 | 0.72 | 0.9 | 0.83 | 0.67 |
| **3** | 0.93 | 0.59 | 0.89 | 0.91 | 0.69 | 0.81 | 0.93 | 0.63 |
| **4** | 0.96 | 0.63 | 0.94 | 0.97 | 0.69 | 0.9 | 0.96 | 0.65 |

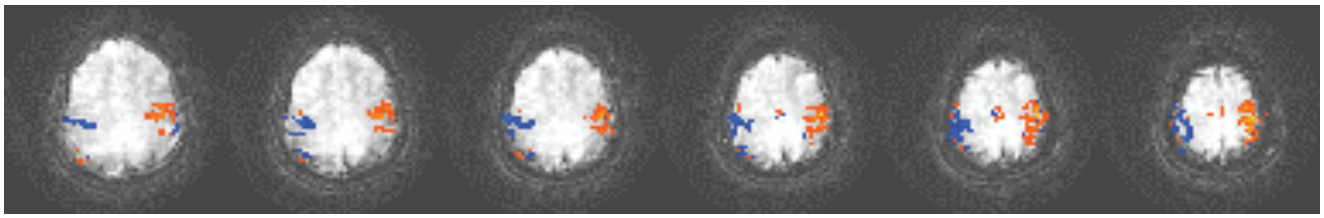

Fig. 1. SVM classification output for the magnitude image data, using alternating right-hand (blue) and left-hand (orange) finger tapping.

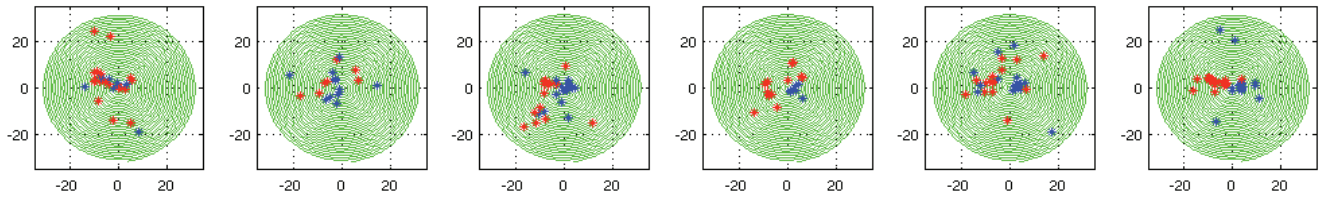


Fig. 2. SVM classification output for the magnitude k-space data, using alternating right-hand (blue) and left-hand (red) finger tapping.

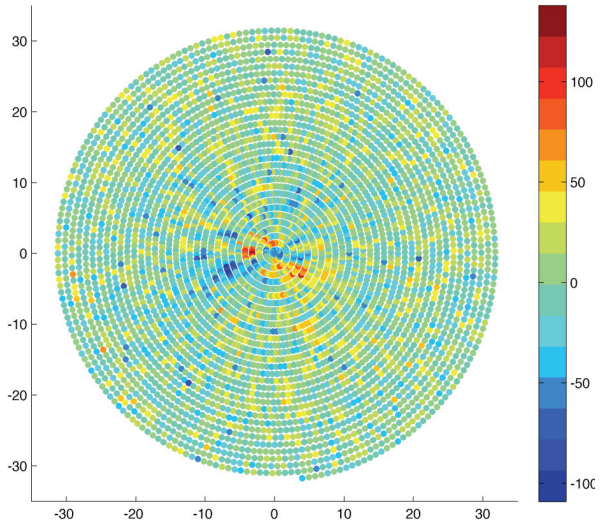


Fig. 3. SVM classification model weights for each k-space point in the spiral acquisition.

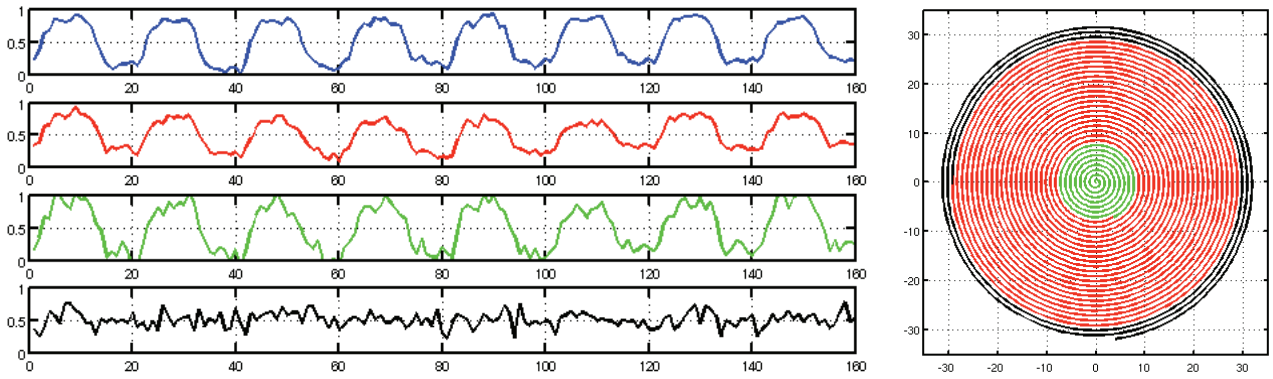

Fig. 4. SVM classification results for a typical subject (1 for left, 0 for right).
(Blue) Magnitude image, (Red) Magnitude k-space, (Green) Magnitude k-space - central 8$^{th}$, (Black) Magnitude k-space - outer 8$^{th}$.